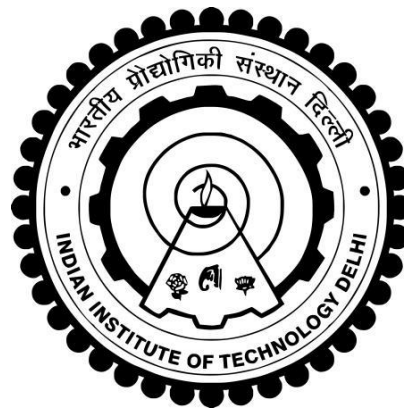


**FAULT TOLERANT SCHEMES FOR EXCHANGING
POWER WITH HVDC TRANSMISSION LINES**

EBIN CHERIAN MATHEW



**DEPARTMENT OF ELECTRICAL ENGINEERING
INDIAN INSTITUTE OF TECHNOLOGY DELHI**

AUGUST 2022

© Indian Institute of Technology Delhi (IITD), New Delhi, 2022

**FAULT TOLERANT SCHEMES FOR EXCHANGING POWER
WITH HVDC TRANSMISSION LINES**

by

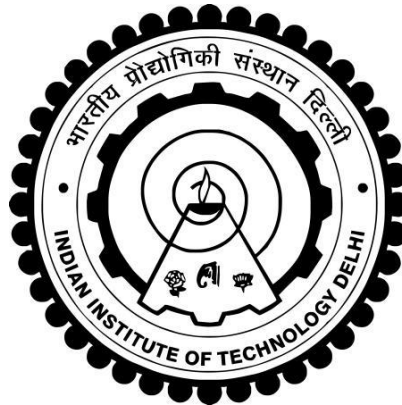
EBIN CHERIAN MATHEW

(Entry No: 2017EEZ8200)

Department of Electrical Engineering

Submitted
in fulfillment of the requirements of the degree of
DOCTOR OF PHILOSOPHY

to the



INDIAN INSTITUTE OF TECHNOLOGY DELHI

August 2022

*I dedicate this thesis to my Creator and beloved Savior,
the Almighty God,
who gave me the intellectual ability to undertake this study.*

CERTIFICATE

This is to certify that the dissertation titled “**FAULT TOLERANT SCHEMES FOR EXCHANGING POWER WITH HVDC TRANSMISSION LINES**”, being submitted by **Mr. Ebin Cherian Mathew** to the Department of Electrical Engineering, Indian Institute of Technology Delhi, for the award of the degree of Doctor of Philosophy, is a record of the bonafide research work carried out by him under my guidance and supervision.

Mr. Ebin Cherian Mathew has fulfilled the requirements for the submission of this thesis, which to my knowledge has reached the requisite standard. The results obtained herein have not been submitted in part or in full to any other University or Institute for the award of any degree.



Dr. Anandarup Das

Department of Electrical Engineering
Indian Institute of Technology Delhi
New Delhi-110016, India

Date: 8/8/2022

ACKNOWLEDGEMENTS

This dissertation has been made possible due to the concerted efforts and encouragement of numerous people. I am deeply grateful to my Lord and Savior Jesus Christ for giving me His grace and helping me through every step during this PhD work.

*First and foremost, I am extremely grateful and remain obliged to my guide **Dr. Anandarup Das, Associate Professor, Department of Electrical Engineering, IIT Delhi** for his constant support and inspiration throughout the PhD. He has always been a guiding spirit to all his students and has always instilled confidence in us. His guidance and vigilant care ensured this work to be transformed from concept to reality. Despite his busy schedule, he always took time to look into the problems faced during this PhD work.*

*My sincere thanks and gratitude to SRC committee members **Dr. G Bhuvanewari, Dr. Amit Kumar Jain, Dr. Sumit Pramanick** and **Dr. Ashu Verma** for their continuous support, supervision, valuable advice, and constructive criticism. This work would not have been possible without their constant mentoring and encouragement.*

*I am ever indebted to my superior officers and colleagues in **Power System Operation Corporation Limited** for their continuous support and guidance. This work would not have been possible without their constant mentoring and encouragement. It would be my utmost pleasure to express my warm thanks to **Sh. Narasimhan S. R, Chairman and Managing Director, Power System Operation Corporation Limited** for his encouragement, cooperation, and consent, without which I would not have been able to accomplish this dissertation. I would like to express my utmost gratitude to my superior officers in Power System Operation Corporation Limited **Sh. Debasis Dey, Sh. Late N. Nallarasan, Sh. Rajeev Porwal, Sh. Surjit Banerjee, Sh. Sajan George, Sh. Vivek Pandey, Sh. Ashok Kumar** and **Sh. Ratnakar Padhy** for giving me constant support for completing my doctoral studies in IIT Delhi. I also express my special thanks to **Sh. Kaushik Dey**, who has been instrumental in constant mentoring and encouragement to complete the PhD.*

*I would like to thank my colleagues, **Dr. Rahul Sharma, Dr. Nibedita Parida, Mrs. Nidhi Bisht** and **Mr. Sukrashis Sarkar** for the discussions, sharing of each other's expertise and experience, helping each other, working together and for all the good times we have had in the last five years.*

*I also express my gratitude to **Ms. Swagata Mapa, Dr. Poonam Jayal, Dr. P. R. Ghosh**, who were instrumental in enabling me to stay committed for the dissertation.*

*I am thankful to all my enthusiastic colleagues for helping me in different ways. Special thanks to **Mr. Rajat Kumar, Mr. Subhasis Nayak and Ms. Cheshta Jain**, for helping me through various stages of my thesis work.*

*My heartfelt thanks goes to my parents, **Mr. Mathew P Cherian & Mrs. Soosy Varghese** for always supporting me that I could focus on my work. I am deeply grateful to my father-in-law, **Mr. Jose C Mathew** and mother-in-law, **Mrs. Saramma J Mathew** for their love, prayers and moral support. I also deeply appreciate the concern and care shown by sister **Dr. Lintu Elsa Mathew** and brother-in-law **Mr. Vivek Varghese**. Special note of thanks to my dear sons, **Joshua Ebin Mathew**, and **Johan Ebin Mathew**, for their ever-beaming faces, which made me forget all the difficulties during the process of this thesis work.*

*I owe thanks to a very special person, my wife, **Dr. Debora J Mathew** for her continued and unfailing love, support and understanding during my pursuit of PhD degree that made completion of this thesis possible. I greatly value her contribution and deeply appreciate her trust in me.*

I thank all who have worked directly and indirectly behind the scenes to make this dissertation possible.

Ebin Cherian Mathew

ABSTRACT

The long-distance power transmission using the HVDC network has been gaining increasing acceptance in recent years. However, in DC transmission, it is challenging to exchange small amount of power from HVDC transmission networks, whereas it can be easily achieved in HVAC transmission networks using simple AC transformers. But there may be many isolated villages/remote renewable energy sources along the route of long-distance HVDC transmission lines which could be integrated into the main power system network. This has attracted industry and academia to explore the possibility of tapping power from HVDC transmission lines and to inject remotely located renewable energy power into HVDC transmission lines. In this thesis, the concept of exchanging a small amount of power from an HVDC transmission line to supply power to isolated rural villages or to integrate remote renewable sources is explored.

A comprehensive literature evaluation of several strategies for exchanging power with HVDC and MVDC transmission lines is presented in Chapter 2. The need for exchanging power from HVDC and MVDC transmission lines is examined. The series and parallel power tapping schemes, as well as the accompanying converter topologies, are thoroughly studied. The difficulties and challenges of transferring power from AC and DC grids with HVDC and MVDC lines are investigated. The requirement of converters used in exchanging power from the DC line is discussed. The concept of direct integration of renewable energy into MVDC grid is also analyzed and various schemes available in the literature are compared.

The power exchange can take place between an HVDC grid and an AC grid. The renewable energy can also be directly integrated to MVDC grid which may be further connected to HVDC transmission line. Suitable converter topologies for the applications are proposed in this thesis. The thesis also investigates the suitability and fault ride through capability of proposed converters in exchanging power from the HVDC transmission line to AC and DC grids.

A new scheme to feed the AC local loads which are near the HVDC transmission corridor using a new DC-DC converter is presented in chapter 3. The proposed DC-DC converter comprises a large number of identical submodules each having one controllable switch, two diodes, and one capacitor. The operation of the DC-DC converter is based on the repeated charging and discharging

of capacitors through a resonant circuit. Zero current switching (ZCS) is achieved for all the switches used in the converter. In case of failure of one submodule, the failed submodule could be bypassed without affecting the normal operation of the HVDC tap. Equations governing the behavior of the proposed converter and the design of the components have been presented. The operational performance of the line commutated converter (LCC) based HVDC system along with the HVDC tapping scheme with the proposed converter is investigated using a simulation model developed in PSCAD/EMTDC. The proposed circuit topology has also been verified with a downscaled experimental prototype.

In Chapter 4, a fault-tolerant scheme for integrating renewable energy sources into a symmetrical monopolar VSC HVDC system using a new modular resonant DC-DC converter is presented. The proposed DC-DC converter consists of many identical low voltage submodules, which consist of two controllable switches, one diode, and a capacitor. The switches of the proposed DC-DC converter are configured to provide the converter with an inherent fault-tolerant feature, which enables it to isolate itself during DC faults in the HVDC system. The integration of renewable energy sources into a symmetrical monopolar VSC HVDC transmission system using the proposed tapping scheme is presented. However, the DC-DC converter has limitations for use in the LCC HVDC system. During the commutation failure/DC side disturbances, the freewheeling diode of the tapping station will conduct thereby feeding power to the inverter HVDC station, thus delaying the recovery of the HVDC system from such disturbances. Thus, the DC-DC converter used for such a power-tapping scheme needs to isolate itself during the DC commutating failures and should not feed the converters of the LCC HVDC system. Thus, a modified modular resonant DC-DC converter is presented to evacuate power to LCC-based HVDC systems. The inherent fault-tolerant capability of the converter prevents it from feeding to any fault in the HVDC line and enables faster recovery from commutation failures in the main HVDC system. The operational performance of the proposed scheme is verified using a simulation model developed in PSCAD/EMTDC and an experimental prototype.

The interconnection of different DC grids is also an active area of research. However, integrating different DC grids, which operate at different voltage levels, configurations, and grounding schemes, has many challenges. The DC distribution grid may also be used for drawing power for EV charging stations and supplying local AC loads. The DC distribution grid may feed

power into the MVDC grid during high renewable power generation and may also need to draw power from the MVDC grid during the low renewable power generation period.

In chapter 5, a new isolated bidirectional hybrid modular DC-DC converter based on a switched-capacitor DC-DC converter for integrating wind farms, solar parks, etc. directly with the MVDC system is presented. The hybrid bidirectional modular converter uses half-bridge submodules in series with a director switch. The converter provides galvanic isolation between DC distribution grid and the MVDC grid. The operation and control strategy of the converter is presented in this chapter. The effectiveness of the converter in exchanging energy between the MVDC grid and the DC distribution grid is validated by the simulation studies performed in PSCAD/EMTDC. The MVDC grid can be further connected to a nearby HVDC grid. A modified isolated hybrid converter using thyristor director switches is also presented in this chapter for HVDC applications.

The power from AC grid can also be directly integrated to an HVDC system. The scheme to integrate a remote AC network with a long-distance LCC-based HVDC system using a full bridge MMC is investigated in first part of chapter 6. The scheme combines the advantages of bulk power transmission capability of Line Commutated Converters and the ability of Voltage Source Converters to connect to a passive network. To achieve DC fault-tolerant capability, the full-bridge Modular Multi-Level Converter (MMC) is used. The coordinated control of the LCC HVDC system with the MMC tapping station is presented. The operational performance of the HVDC system with the MMC-based shunt tap and its performance during DC side fault is analyzed using the time domain simulation model developed in PSCAD/EMTDC.

In second part of chapter 6, a new scheme to directly integrate the output of wind generators and solar PV panels with an MVDC system is presented. The DC-DC converter proposed in chapter 4 is used for the integration scheme. The scheme will reduce the number of equipment involved in the energy conversion process. In the scheme presented in this chapter, the output of a permanent magnet synchronous generator coupled with a wind turbine is converted to a low voltage DC by an AC-DC converter and then directly connected to an MVDC system using the fault tolerant soft switched high gain DC-DC converter. The output from high voltage solar PV panels is also connected with the MVDC transmission network with the DC-DC converter. The integration of wind turbines/solar PV panels with the MVDC system using the proposed scheme is verified using extensive simulation studies done in PSCAD/EMTDC. A new scheme to bypass

the faulty MVDC corridor by using simple DC disconnectors is also presented in chapter 6. The working principle and operation of converter is also verified with experimental results.

The conclusion and future scope of work are discussed in chapter 7. The method of tapping power from the HVDC system is still in the early stages of research and development and further research is required for its commercial implementation.

सार

हाल के वर्षों में एच.वी.डी.सी. नेटवर्क का उपयोग करते हुए लंबी दूरी की विद्युत पारेषण की स्वीकार्यता बढ़ रही है। हालांकि, कम मात्रा में बिजली का आदान-प्रदान करना एच.वी.डी.सी. ट्रांसमिशन नेटवर्क से चुनौतीपूर्ण है, जबकि इसे साधारण एच.वी.ए.सी. ट्रांसमिशन नेटवर्क में ए.सी. ट्रांसफार्मर का उपयोग करके आसानी से प्राप्त किया जा सकता है। लेकिन लंबी दूरी की एच.वी.डी.सी. ट्रांसमिशन लाइनों के मार्ग के साथ कई अलग-अलग गांव/दूरस्थ नवीकरणीय ऊर्जा स्रोत हो सकते हैं जिन्हें मुख्य बिजली प्रणाली नेटवर्क में एकीकृत किया जा सकता है। इसने उद्योग और शिक्षाविदों को एच.वी.डी.सी. ट्रांसमिशन लाइनों से बिजली के दोहन की संभावना का पता लगाने और दूर से स्थित अक्षय ऊर्जा शक्ति को एच.वी.डी.सी. ट्रांसमिशन लाइनों में इंजेक्ट करने के लिए आकर्षित किया है। इस थीसिस में, अलग-अलग ग्रामीण गांवों को बिजली की आपूर्ति करने या दूरस्थ नवीकरणीय स्रोतों को एकीकृत करने के लिए एच.वी.डी.सी. ट्रांसमिशन लाइन से थोड़ी मात्रा में बिजली का आदान-प्रदान करने की अवधारणा का पता लगाया गया है।

एच.वी.डी.सी. और एम.वी.डी.सी. ट्रांसमिशन लाइनों के साथ बिजली के आदान-प्रदान के लिए कई रणनीतियों का एक व्यापक साहित्य मूल्यांकन अध्याय 2 में प्रस्तुत किया गया है। एच.वी.डी.सी. और एम.वी.डी.सी. ट्रांसमिशन लाइनों से बिजली के आदान-प्रदान की आवश्यकता की जांच की गयी है। सीरीज़ और पैरेलल बिजली दोहन योजनाओं का, साथ ही साथ कनवर्टर टोपोलॉजीओं का गहन अध्ययन किया गया है। एच.वी.डी.सी. और एम.वी.डी.सी. लाइनों के साथ ए.सी. और डी.सी. ग्रिड से बिजली स्थानांतरित करने की कठिनाइयों और चुनौतियों की जांच की गयी है। डी.सी. लाइन से बिजली के आदान-प्रदान में प्रयुक्त कन्वर्टर की आवश्यकता पर चर्चा की गई है। एम.वी.डी.सी. ग्रिड में अक्षय ऊर्जा के प्रत्यक्ष एकीकरण की अवधारणा का भी विश्लेषण किया गया है और साहित्य में उपलब्ध विभिन्न योजनाओं की तुलना की गयी है।

पावर एक्सचेंज एच.वी.डी.सी. ग्रिड और ए.सी. ग्रिड के बीच हो सकता है। अक्षय ऊर्जा को सीधे एम.वी.डी.सी. ग्रिड से भी जोड़ा जा सकता है जिसे आगे एच.वी.डी.सी. ट्रांसमिशन लाइन से जोड़ा जा सकता है। इस थीसिस में अनुप्रयोगों के लिए उपयुक्त कनवर्टर टोपोलॉजी प्रस्तावित हैं। थीसिस एच.वी.डी.सी. ट्रांसमिशन लाइन से ए.सी. और डी.सी. ग्रिड में बिजली के आदान-प्रदान में प्रस्तावित कन्वर्टर की क्षमता के माध्यम से उपयुक्तता और दोष-सहिष्णु योजना प्रस्तुत की गई है।

एक नए डी.सी.-डी.सी. कनवर्टर का उपयोग करके एच.वी.डी.सी. ट्रांसमिशन कॉरिडोर के पास स्थानीय ए.सी. लोड को फिड करने के लिए एक नई योजना अध्याय 3 में प्रस्तुत की गई है। प्रस्तावित डी.सी.-डी.सी.

कनवर्टर में बड़ी संख्या में समान सबमॉड्यूल शामिल हैं जिनमें से प्रत्येक में एक नियंत्रणीय स्विच, दो डायोड और एक संधारित्र हैं। डी.सी.-डी.सी. कनवर्टर का संचालन एक अनुनाद सर्किट के माध्यम से कैपेसिटर के बार-बार चार्ज और डिस्चार्जिंग पर आधारित होता है। कनवर्टर में उपयोग किए जाने वाले सभी स्विच के लिए जीरो करंट स्विचिंग हासिल की गई है। एक सबमॉड्यूल की विफलता के मामले में, एच.वी.डी.सी. टैप के सामान्य संचालन को प्रभावित किए बिना विफल सबमॉड्यूल को बायपास किया जा सकता है।

प्रस्तावित कनवर्टर के व्यवहार और घटकों के डिजाइन को नियंत्रित करने वाले समीकरण प्रस्तुत किए गए हैं। प्रस्तावित कनवर्टर के साथ एच.वी.डी.सी. टैपिंग योजना के साथ लाइन कम्प्यूटेड कनवर्टर (एल.सी.सी.) आधारित एच.वी.डी.सी. प्रणाली के परिचालन प्रदर्शन की जांच पी.एस.सी.ए.डी./ई.एम.टी.डी.सी. में विकसित सिमुलेशन मॉडल का उपयोग करके की गई है। प्रस्तावित सर्किट टोपोलॉजी को भी एक डाउनस्केल प्रायोगिक प्रोटोटाइप के साथ सत्यापित किया गया है।

अध्याय 4 में, एक नए मॉड्यूलर अनुनाद डी.सी.-डी.सी. कनवर्टर का उपयोग कर एक सममित मोनोपोलर वी.एस.सी. एच.वी.डी.सी. प्रणाली में अक्षय ऊर्जा स्रोतों को एकीकृत करने के लिए एक दोष-सहिष्णु योजना प्रस्तुत की गई है। प्रस्तावित डी.सी.-डी.सी. कनवर्टर में कई समान कम वोल्टेज सबमॉड्यूल होते हैं, जिसमें दो नियंत्रणीय स्विच, एक डायोड और एक संधारित्र है। प्रस्तावित डी.सी.-डी.सी. कनवर्टर के स्विच को एक अंतर्निहित दोष-सहिष्णु सुविधा के साथ कनवर्टर प्रदान करने के लिए कॉन्फ़िगर किया गया है, जो इसे एच.वी.डी.सी. सिस्टम में डी.सी. दोषों के दौरान खुद को अलग करने में सक्षम बनाता है। प्रस्तावित टैपिंग योजना का उपयोग करते हुए एक सममित मोनोपोलर वी.एस.सी. एच.वी.डी.सी. ट्रांसमिशन सिस्टम में अक्षय ऊर्जा स्रोतों का एकीकरण प्रस्तुत किया गया है। हालाँकि, डी.सी.-डी.सी. कनवर्टर की एल.सी.सी. एच.वी.डी.सी. प्रणाली में उपयोग की सीमाएँ हैं। कम्प्यूटेशन फेल होने/डी.सी. साइड डिस्टर्बेंस के दौरान, टैपिंग स्टेशन का फ्रीव्हीलिंग डायोड इन्वर्टर एच.वी.डी.सी. स्टेशन को फ्रीडिंग पावर का संचालन करेगा, इस प्रकार एच.वी.डी.सी. सिस्टम को इस तरह की गड़बड़ी से उबरने में देरी होगी। इस प्रकार, इस तरह की पावर-टैपिंग योजना के लिए उपयोग किए जाने वाले डी.सी.-डी.सी. कनवर्टर को डी.सी. दोषों के दौरान खुद को अलग करने की जरूरत है और एल.सी.सी. एच.वी.डी.सी. सिस्टम के कन्वर्टर्स को फीड नहीं करना चाहिए। इस प्रकार, एल.सी.सी.-आधारित एच.वी.डी.सी. सिस्टम को बिजली निकालने के लिए एक संशोधित मॉड्यूलर अनुनाद डी.सी.-डी.सी. कनवर्टर प्रस्तुत किया गया है। कनवर्टर की अंतर्निहित दोष-सहिष्णु क्षमता एच.वी.डी.सी. लाइन में किसी भी फॉल्ट को फीड करने से रोकती है और मुख्य एच.वी.डी.सी. प्रणाली में कम्प्यूटेशन विफलताओं से तेजी से वसूली को सक्षम बनाती है। पी.एस.सी.ए.डी./ई.एम.टी.डी.सी. में विकसित

सिमुलेशन मॉडल और एक प्रयोगात्मक प्रोटोटाइप का उपयोग करके प्रस्तावित योजना के परिचालन प्रदर्शन को सत्यापित किया गया है।

विभिन्न डी.सी. ग्रिड का इंटरकनेक्शन भी अनुसंधान का एक सक्रिय क्षेत्र है। हालांकि, विभिन्न डी.सी. ग्रिड को एकीकृत करना, जो विभिन्न वोल्टेज स्तरों, कॉन्फिगरेशन और ग्राउंडिंग योजनाओं पर काम करते हैं, में कई चुनौतियां हैं। डी.सी. वितरण ग्रिड का उपयोग ई.वी. चार्जिंग स्टेशनों के लिए बिजली खींचने और स्थानीय ए.सी. लोड की आपूर्ति के लिए भी किया जा सकता है। डी.सी. वितरण ग्रिड उच्च नवीकरणीय बिजली उत्पादन के दौरान एम.वी.डी.सी. ग्रिड में बिजली फिड कर सकता है और कम नवीकरणीय बिजली उत्पादन अवधि के दौरान एम.वी.डी.सी. ग्रिड से बिजली खींचने की भी आवश्यकता हो सकती है।

अध्याय 5 में, एम.वी.डी.सी. प्रणाली के साथ सीधे पवन खेतों, सौर पार्कों आदि को एकीकृत करने के लिए स्विच-कैपेसिटर डी.सी.-डी.सी. कनवर्टर पर आधारित एक नया पृथक द्विदिश हाइब्रिड मॉड्यूलर डी.सी.-डी.सी. कनवर्टर प्रस्तुत किया गया है। हाइब्रिड द्विदिश मॉड्यूलर कनवर्टर एक निर्देशक स्विच के साथ सीरीज़ में हाफ-ब्रिज सबमॉड्यूल का उपयोग करता है। कनवर्टर डी.सी. वितरण ग्रिड और एम.वी.डी.सी. ग्रिड के बीच गैल्वेनिक अलगाव प्रदान करता है। कनवर्टर के संचालन और नियंत्रण की रणनीति इस अध्याय में प्रस्तुत की गई है। एम.वी.डी.सी. ग्रिड और डी.सी. वितरण ग्रिड के बीच ऊर्जा के आदान-प्रदान में कनवर्टर की प्रभावशीलता पी.एस.सी.ए.डी/ई.एम.टी.डी.सी. में किए गए सिमुलेशन अध्ययनों द्वारा मान्य है। एम.वी.डी.सी. ग्रिड को पास के एच.वी.डी.सी. ग्रिड से जोड़ा जा सकता है। एच.वी.डी.सी. अनुप्रयोगों के लिए इस अध्याय में थाइरिस्टर निदेशक स्विच का उपयोग कर एक संशोधित पृथक हाइब्रिड कनवर्टर भी प्रस्तुत किया गया है। प्रस्तावित सर्किट टोपोलॉजी को भी एक डाउनस्केल प्रायोगिक प्रोटोटाइप के साथ सत्यापित किया गया है।

ए.सी. ग्रिड से बिजली को सीधे एच.वी.डी.सी. सिस्टम में भी एकीकृत किया जा सकता है। एक फुल-ब्रिज एम.एम.सी. का उपयोग करके एक लंबी दूरी की एल.सी.सी.-आधारित एच.वी.डी.सी. प्रणाली के साथ एक दूरस्थ ए.सी. नेटवर्क को एकीकृत करने की योजना की जांच अध्याय 6 के पहले भाग में की गई है। यह योजना लाइन कम्प्यूटेटेड कन्वर्टर्स की बल्क पावर ट्रांसमिशन क्षमता और एक निष्क्रिय नेटवर्क से जुड़ने के लिए वोल्टेज सोर्स कन्वर्टर्स की क्षमता को जोड़ती है। डी.सी. दोष-सहिष्णु क्षमता प्राप्त करने के लिए, फुल-ब्रिज मॉड्यूलर मल्टी-लेवल कन्वर्टर (एम.एम.सी.) का उपयोग किया गया है। एम.एम.सी. टैपिंग स्टेशन के साथ एल.सी.सी. एच.वी.डी.सी. प्रणाली का समन्वित नियंत्रण प्रस्तुत किया गया है। एम.एम.सी.-आधारित शंट टैप के साथ एच.वी.डी.सी. प्रणाली के परिचालन प्रदर्शन और डी.सी. साइड फॉल्ट के दौरान इसके प्रदर्शन

का विश्लेषण पी.एस.सी.ए.डी./ई.एम.टी.डी.सी. में विकसित टाइम डोमेन सिमुलेशन मॉडल का उपयोग करके किया गया है।

अध्याय 6 के दूसरे भाग में, एम.वी.डी.सी. प्रणाली के साथ पवन जनरेटर और सौर पी.वी. पैनलों के उत्पादन को सीधे एकीकृत करने की एक नई योजना प्रस्तुत की गई है। डी.सी.-डी.सी. कनवर्टर अध्याय 4 में प्रस्तावित एकीकरण योजना के लिए प्रयोग किया गया है। यह योजना ऊर्जा रूपांतरण प्रक्रिया में शामिल उपकरणों की संख्या को कम करेगी। इस अध्याय में प्रस्तुत योजना में, पवन टरबाइन के साथ युग्मित स्थायी चुंबक तुल्यकालिक जनरेटर के आउटपुट को ए.सी.-डी.सी. कनवर्टर द्वारा कम वोल्टेज डी.सी. में परिवर्तित किया गया है और फिर फॉल्ट टॉरेंट सॉफ्ट स्विच हाई गेन का उपयोग करके सीधे एम.वी.डी.सी. सिस्टम से जोड़ा गया है। डी.सी.-डी.सी. कनवर्टर उच्च वोल्टेज सौर पीवी पैनलों से आउटपुट डी.सी.-डी.सी. कनवर्टर के साथ एम.वी.डी.सी. ट्रांसमिशन नेटवर्क से भी जुड़ा हुआ है। प्रस्तावित योजना का उपयोग करते हुए एम.वी.डी.सी. प्रणाली के साथ पवन टरबाइन/सौर पी.वी. पैनलों का एकीकरण पी.एस.सी.ए.डी./ई.एम.टी.डी.सी. में किए गए व्यापक सिमुलेशन अध्ययनों का उपयोग करके सत्यापित किया गया है। साधारण डी.सी. डिस्कनेक्टर्स का उपयोग करके दोषपूर्ण एम.वी.डी.सी. कॉरिडोर को बायपास करने के लिए एक नई योजना भी अध्याय 6 में प्रस्तुत की गई है।

कार्य के निष्कर्ष और भविष्य के दायरे पर अध्याय 7 में चर्चा की गई है। एच.वी.डी.सी. प्रणाली से शक्ति के दोहन की विधि अभी भी अनुसंधान और विकास के प्रारंभिक चरण में है और इसके वाणिज्यिक कार्यान्वयन के लिए और अनुसंधान की आवश्यकता है।

TABLE OF CONTENTS

Certificate	i
Acknowledgments	iii
Abstract	v
Abstract (Hindi)	ix
Table of Contents	xiii
List of Figures	xvi
List of Tables	xxv
List of Abbreviations	xxvi
List of Symbols	xxvii

Chapter 1 Introduction	1-8
1.1 Background and Motivation of the Work	1
1.2 Research Gap Identification	2
1.3 Main Contributions of the Thesis	3
1.4 Organization of the Thesis	5

Chapter 2 Literature Review	9-51
2.1 Need for HVDC Power Tapping	10
2.2 Classification of HVDC systems	11
2.3 Concept of HVDC power tapping	18
2.4 Classification of Power Tapping schemes	19
2.5 Series power tapping scheme	20
2.5.1 Existing topologies for series power tapping scheme	21
2.5.2 Challenges with series power tapping schemes	24
2.6 Parallel tapping scheme	25
2.6.1. Single-stage HVDC parallel tapping scheme.	26
2.6.2. Two-stage HVDC parallel tapping scheme.	30
2.7 DC-DC converters for HVDC power tapping schemes	31
2.7.1. Non-Isolated topologies.	31
2.7.2. Isolated topologies	37
2.8 Operational challenges of tapping power from HVDC lines	41
2.8.1. Response to AC and DC side disturbances	41
2.8.2. Operation of tapping station during DC and AC side faults	42
2.8.3. Operational aspects of tapping stations	43
2.9 Integration of renewable energy sources with DC grid	44
2.9.1. Limitations of AC collection platform	45
2.9.2. Integration of renewable energy with DC collection platforms.	45
2.10 Research Area Identification	48

Chapter 3 DC-DC Converter Topology for tapping power from HVDC system	52-76
3.1 Proposed power tapping scheme	53
3.1.1 Configuration of tapping scheme	53

	3.1.2 Proposed submodule structure.	54
	3.1.3 Operating principle	54
	3.1.4 Mathematical analysis of the DC-DC converter	56
	3.1.5 Configurations of the bypass switch.	60
	3.1.6 Derived submodule structures	61
	3.1.7 Design of the DC-DC Converter	63
	3.1.8 Operation of the converter with variable voltage conversion ratio.	63
	3.1.9 Combined operation of multiple DC-DC Converter	65
3.2	Simulation results	69
3.3	Experimental results	75
3.4	Summary	78

Chapter 4 DC-DC Converter Topologies for Evacuation of Renewable Power to HVDC system		79-122
4.1	Power evacuation scheme with DC-DC converter topology-1	79
	4.1.1. Configuration of power evacuation scheme	81
	4.1.2. Operation of the DC-DC converter.	82
	4.1.3. DC Fault ride-through capability of the power evacuation scheme	86
	4.1.4 Design of the DC-DC Converter	90
	4.1.5. Simulation results.	91
	4.1.6. Experimental Results.	97
4.2	Power evacuation scheme with DC-DC converter topology-2	100
	4.2.1. Configuration of power evacuation scheme.	101
	4.2.2. Operation of the DC-DC converter.	102
	4.2.3. Steady-state analysis of the converter	104
	4.2.4. Analysis of LCC HVDC system with power tapping scheme	110
	4.2.5 Design of the DC-DC Converter	113
	4.2.6. Simulation results.	114
	4.2.7. Experimental Results.	121
4.3	Summary	124

Chapter 5 Isolated bidirectional hybrid DC-DC converter topologies for exchanging power with the DC grid.		126-155
5.1	Isolated DC-DC converter for exchanging power with Bipolar DC grid	129
	5.1.1. Converter configuration.	130
	5.1.2 Converter operation	132
	5.1.3 Mathematical analysis of converter topology.	134
	5.1.4 Control of the converter.	136
	5.1.5. Simulation results	137
5.2	Isolated DC-DC converter for exchanging power with Monopolar DC grid	142
	5.2.1 Converter configuration	142
	5.2.2. Converter operation	143
	5.2.3 Simulation results	146

5.3	Modified DC-DC converter using thyristor valves for interconnecting HVDC and MVDC grid	146
	5.3.1. Modified Converter configuration.	147
	5.3.2 Converter operation.	150
	5.3.3 Mathematical Analysis of the Converter Operation	151
	5.3.4 Capacitor Voltage Insertion Strategy	154
	5.3.5 Simulation And Experimental results	157
5.4	Summary	163

Chapter 6 AC and DC collection platforms for integration of renewable energy sources		164-191
6.1	Integrating the AC collection platform into the HVDC system	166
	6.1.1. Requirement of AC-DC converters for integrating AC collection platform with HVDC line	167
	6.1.2. System configuration	169
	6.1.3. Dynamic Control of LCC HVDC system connected to an AC collection platform	170
	6.1.4. Start-up of MMC connected to AC collection platform	172
	6.1.5. DC fault analysis of LCC HVDC system with MMC connected to AC collection platform	173
	6.1.6. Simulation Results	174
	6.1.7. Summary	176
6.2	Integrating the DC collection platform into the MVDC system	176
	6.2.1. Direct integration of renewable resources to the MVDC grid.	177
	6.2.2 Wind turbine integration	179
	6.2.3 Solar PV panel integration	180
	6.2.4 Configuration of DC collection platform	183
	6.2.5 Control of DC collection platform	183
	6.2.6 DC Fault ride through capability	186
	6.2.7 Simulation results	187
	6.2.8 Summary.	192
6.3	Conclusion	193

Chapter 7 Conclusion and Future Scope of Work		194-195
7.1	Summary of the Research	194
7.2	Future Scope	194

REFERENCES		196-205
APPENDIX-A: LIST OF PUBLICATIONS		206
APPENDIX-B: Curriculum Vitae		207

LIST OF FIGURES

1.1	Schemes to exchange power with HVDC transmission line
2.1	Operating configurations of HVDC system
2.2	Power flow in HVDC system with a) Series tapping scheme b) Parallel tapping scheme
2.3 (a)	Classification of HVDC power tapping schemes
2.3 (b)	Power electronic based power tapping schemes (i) Series power tapping scheme (ii) Parallel power tapping scheme (Single stage) (iii) Parallel power tapping scheme (Two stage) using a DC-DC converter.
2.4	Series power tapping scheme
2.5	Series tapping scheme proposed in [27]
2.6	Series tapping scheme proposed in [28]
2.7	Series power tapping with CSC converter [29]
2.8	Series tapping scheme with modular multilevel converters [30]
2.9	HVDC series tapping using M2CSC [32],
2.10	n-phase multinodular series tap (MMST) presented in [33]
2.11	Parallel power tapping scheme
2.12	Parallel power tap with VSC HVDC system [34]
2.13	Parallel power tap with VSC HVDC system [35].
2.14	Equivalent circuit of Hybrid HVDC system during commutation failure [35]
2.15	Tap for Classical HVDC Based on Multilevel Current-Source Inverters [36]
2.16	Tapping existing LCC-HVDC systems with Voltage Source Converters [37]
2.17	Tapping HVDC transmission line using a three-phase series-connected hybrid modular multilevel converter [45]
2.18	Two-stage power tapping scheme
2.19	Classification of DC-DC converters
2.20	Modular DC-DC converter [57]
2.21	HVDC parallel tap based on unidirectional hybrid modular DC-DC converter [59]
2.22	Step-up Resonant Converter for Grid-Connected Renewable Energy Sources [60]
2.23	High-power DC transformer [61]
2.24	High Power Resonant Switched-Capacitor Step-Down Converter [60]
2.25	Marx DC-DC converter topology presented in [68]
2.26	Scalable DC-DC converter based on Marx concept [69]- [70]
2.27	Hybrid-Cascaded DC-DC Converters Suitable for HVDC Applications [79]- [80]
2.28	(a) DC-DC converter without galvanic isolation (b) DC-DC converter without galvanic isolation
2.29	Isolated DC/DC structure based on modular multilevel converter [88]
2.30	Isolated DC/DC structure using transition arm modular multilevel converter [89]

2.31	Isolated DC/DC converter using Hybrid TAC structure. [90]
2.32	Isolated Resonant Mode Modular Converter [91]
2.33	Direct integration of renewable energy sources with MVDC network
2.34	Series connected wind turbine system
2.35	Parallel connected wind turbine system
3.1	Scheme to tap power from HVDC system with proposed DC-DC converter
3.2	Proposed submodule structure (Type A and Type B)
3.3	Charging of DC -DC converter (indicated by green line)
3.4	Equivalent circuit during charging.
3.5	Discharging of DC -DC converter (indicated by green line)
3.6	Equivalent circuit during discharging.
3.7	Equivalent circuit during charging.
3.8	Charging of DC-DC converter: (a) charging current ($I_c(t)$). (b) HVDC transmission line voltage (V_g) and voltage across the series connected submodule capacitors ($V_c(t)$)
3.9	Equivalent circuit during discharging
3.10	Discharging of DC-DC converter (a) Discharging current ($I_d(t)$). (b) VSC capacitor voltage ($V_o(t)$) and voltage across the parallel connected submodule capacitors ($V_{sm}(t)$).
3.11	Type 1-Implementation of Bypass switch.
3.12	Type-2-Implementation of Bypass switch.
3.13	Modified topology with inductor in series with submodule capacitor (i) Topology-1 (ii) Topology-2
3.14	Modified topology with inductor in the parallel charging path (i) Topology-1 (ii) Topology-2
3.15	Equivalent circuit of the scheme shown in Fig 4.1 with modified submodule topology (Fig.4.13 (i))
3.16	Equivalent circuit of the scheme shown in Fig 4.1 with modified submodule topology (Fig.4.13 (ii))
3.17	Combined operation of multiple DC-DC Converter
3.18	Current drawn from HVDC transmission line during combined operation of multiple DC-DC converter
3.19	Steady-state converter waveforms during the discharging process of submodule capacitors (C_{sm}) to output capacitor (C_o).
3.20	Steady-state performance of proposed power tapping scheme
3.21	Response of the converter to the step-change in Input voltage from 500kV to 400kV at t=3sec
3.22	Operation of DC-DC converter during the dynamic change in tapped power from 80MW to 150 MW at t=5 sec
3.23	Dynamic Performance of HVDC system with the change in tapped power from 80MW to 150 MW at t=5 sec
3.24	Dynamic Performance of HVDC system with the change in tapped power from 80MW to 150 MW at t=5 sec.
3.25	Response of the proposed system during a pole to ground fault in the HVDC line at t=3sec

3.26	Experimental prototype
3.27	Experimental results showing: (i) step down operation of DC-DC
3.27	Experimental results showing: (ii) Resonant operation of discharging circuit (iii) Resonant operation of charging circuit
3.28	Experimental results showing charging and discharging of the DC-DC converter
3.29	Experimental results showing Zero current switching of director switch (S_{HVP})
3.30	Experimental results showing individual submodule capacitor voltages in the upper arm of the DC-DC converter
4.1	Scheme to evacuate power to HVDC system with the proposed DC-DC converter Topology-1
4.2	Proposed submodule structure (Type A and Type B)
4.3	Charging of DC-DC converter from VSC
4.4	Equivalent circuit of the proposed converter during charging
4.5	Discharging of DC-DC converter to HVDC transmission line
4.6	Equivalent circuit of the proposed converter during discharging
4.7	Scheme to limit the ripple in the current injected to HVDC line
4.8	Equivalent circuit of a symmetrical monopole MMC based HVDC system with the proposed scheme during DC side fault
4.9	Equivalent circuit of HVDC system with proposed tapping scheme during stage-1 (Before blocking the MMC and DC-DC converter)
4.10	Equivalent circuit of MMC HVDC system with proposed tapping scheme during stage-2 (After blocking the MMC and DC-DC converter but before opening AC circuit breaker)
4.11	Equivalent circuit of MMC HVDC system with proposed tapping scheme during stage-3 (After opening AC circuit breaker)
4.12	Equivalent circuit of symmetrical monopolar MMC HVDC system during pole to ground fault
4.13	Steady-state converter waveforms showing step-up operation of DC-DC converter (a) HVDC grid voltage- V_{HVDC} (kV) (b) Input voltage, $V_{VSC}(t)$ (kV) (c) Current injected to HVDC transmission line- $I_{line}(t)$ - (kA) (d) Total power injected to HVDC system (MW).
4.14	Steady-state converter waveforms showing charging of submodules from renewable energy source (a) Input Voltage- $V_{VSC}(t)$ (kV) and Voltage across submodule capacitor- $V_{sm}(t)$ (kV) (b) Voltage across input inductor (L_{in}) (kV) (c) Charging current- $I_c(t)$ (kA).
4.15	Steady-state converter waveforms during discharging process of DC-DC converter to HVDC system: (a) HVDC voltage (V_{HVDC}) and Voltage across series connected submodule capacitors ($V_c(t)$) (kV) (b) Voltage across output inductor (L_o) (kV) (c) Discharging Current- $I_d(t)$ (kA).
4.16	Steady-state converter waveforms during evacuation of power from renewable energy sources through DC-DC converter to HVDC system: (a) Current injected to the HVDC transmission line (I_{line}) (b) HVDC

	voltage (V_{HVDC}) (c) Power injected by the HVDC tap to the HVDC system (d) Power send by rectifier HVDC station (P_r) and Power received by inverter HVDC station (P_i)
4.17	Performance of the converter during the DC Pole to Pole fault applied at $t=5$ sec. (a) HVDC transmission line voltage- V_{HVDC} (kV): (Positive pole (V_{pg}) and Negative pole (V_{ng}) (b) Current injected to HVDC system from the DC-DC converter (kA) (kV) (c) AC current drawn by rectifier station of HVDC system (d) DC Fault current (e) Voltage across submodule capacitor- $V_{sm}(t)$ (kV)
4.18	Performance of the converter during the DC pole to ground fault applied at $t=5$ sec. (a) HVDC Voltage- V_{HVDC} : (Positive pole (V_{pg}) and Negative pole (V_{ng}) (kV) (b) Current injected to HVDC system from the DC-DC converter (kA) (c) AC current drawn by rectifier of HVDC link (kA) (d) DC Fault current (kA) (e) Voltage across submodule capacitor- $V_{sm}(t)$ (kV)
4.19	Experimental results showing: (a) step up operation of DC-DC converter (b) Resonant operation of charging circuit (c) Resonant operation of discharging circuit
4.20	Experimental results showing the resonance operation of the charging circuit
4.21	Experimental results showing the resonance operation of discharging circuit
4.22	Experimental results showing: (a) Uniform charging and discharging of submodule capacitors
4.23	Experimental results showing Zero current switching of switch S_1
4.24	Experimental results showing Zero current switching of switch S_2
4.25	Limitation of DC-DC converter topology-1 in evacuating power to LCC HVDC system.
4.26	Proposed scheme to evacuate power from the remote renewable energy sources to HVDC grid.
4.26	Proposed submodule configuration (Type A and Type B)
4.28	Switching states of the proposed DC-DC converter (Indicated by blue line)
4.29	Equivalent circuit of the proposed scheme during charging.
4.30	Equivalent circuit of the proposed scheme during discharging
4.31	Over control structure of the proposed system.
4.32 (i)	DC Fault ride through capability of the proposed scheme during pole to ground fault at positive pole (DC-DC converter blocked)
4.32 (ii)	Equivalent circuit during a) stage-1 of DC fault b) stage-2 of DC fault
4.33	Steady-state converter waveforms showing step-up operation of DC-DC converter (a) HVDC grid voltage- V_g (kV) (b) Input voltage, $V_{in}(t)$ (kV) (c) Current injected to HVDC transmission line (kA) (d) Total power injected to the HVDC system through the DC-DC converter (MW).
4.34	Simulation results showing charging of submodules from renewable energy source (a) Input Voltage- $V_{in}(t)$ (kV) and Voltage across submodule capacitor- $V_{sm}(t)$ (kV) (b) Voltage across input inductor (kV) (c) Charging current- $I_c(t)$ (kA).
4.35	Simulation results showing discharging process of DC-DC converter to HVDC system: (a) HVDC voltage (V_g) and total voltage across series connected submodule capacitors ($V_c(t)$) (kV) (b) Voltage across output inductor (kV) (c) Discharging current- $I_d(t)$ (kA).

4.36	Simulation results showing steady state operation of DC-DC converter in LCC based HVDC system: (a) HVDC voltage (V_g) (b) Rectifier current (I_r)-kA and Inverter current (I_i)-kA (c) Current injected to HVDC system (kA). (d) Rectifier firing angle (α) and Inverter extinction angle (γ) (deg) (e) Power send from rectifier (P_r) and Power received at inverter (P_s) (f) Power injected to HVDC system by DC-DC converter
4.37	Simulation results showing steady state operation of DC-DC converter in LCC based HVDC system: (a) HVDC voltage (V_g) (b) Rectifier current (I_r)-kA and Inverter current (I_i)-kA (c) Current injected to HVDC system (kA). (d) Fault current (kA) (e) Rectifier firing angle (α) and Inverter extinction angle (γ) (deg) (f) DC-DC converter submodule capacitor voltage- V_{sm} (kV)
4.38	Fig. 5.38 Simulation results showing steady state operation of DC-DC converter in LCC based HVDC system: (a) HVDC voltage (V_g) (b) Rectifier current (I_r)-kA and Inverter current (I_i)-kA (c) Current injected to HVDC system (kA). (d) Inverter AC voltage (kA) (e) Rectifier firing angle(α) (°) and Inverter extinction angle(γ) (°) (deg) (f) DC-DC converter submodule capacitor voltage- V_{sm} (kV).
4.39	Experimental prototype built in lab
4.40	Experimental results showing step up operation of DC-DC converter. (a) Charging current (10A/div) (b) Input voltage (50V/div) (c) Output voltage (200V/div) (d) Load current (500mA/div).
4.41	Experimental results showing resonant charging and discharging process. (a) Charging current (10A/div) (b) Voltage across input inductance (20V/div) (c) Discharging current (2A/div) (d) Voltage across output inductance (20V/div)
4.42	Experimental results showing: (i) Zero current switching of switch S1 and S2 in submodule (SP1) (a) Voltage across switch S1 (50V/div) (b) Current through switch S1 (10A/div) (c) Voltage across switch S2 (50V/div) (d) Current through switch S2 (2A/div)
4.43	Experimental results showing Voltage across and current through blocking diodes DP and DN (a) Current through Diode DP (2A/div) (b) Voltage across Diode DP (200V/div) (d) Current through Diode DN (2A/div) (d) Voltage across Diode DN (200V/div)
4.44	Experimental results showing uniform charging and discharging of submodule capacitors (20V/div).
4.45	Experimental results showing response of the DC-DC converter during DC fault: (a) Submodule capacitor voltage (30V/div) (b) Output current (2A/div) (c) Gate pulse to switch S2 (50V/div) (d) Input current (10A/div)
4.46	Experimental results showing response of the DC-DC converter during DC fault (a) Output DC voltage (50V/div) (b) Submodule capacitor voltage (50V/div) (c) Gate pulse to switch S ₁ (20V/div) (d) Gate pulse to switch S ₂ (20V/div) (
4.47	Experimental results showing response of the DC-DC converter during DC fault: Voltage across submodule capacitor (50V/div) (a) SM ₁ (b) SM ₂ (c) SM ₃ (d) SM ₄
5.1	General schematic of the DC distribution grid connected to an HVDC grid through an MVDC grid.
5.2	Isolated hybrid modular DC-DC converter

5.3	Voltage generated by wave shaping circuit across isolation transformer (kV) (Power flow from high to low voltage side)
5.4	Voltage generated by wave shaping circuit across isolation transformer (kV) (Power flow from low to high voltage side)
5.5	Illustration of charging and discharging of the isolated DC-DC converter topology (Power flow from HV to LV side)
5.6	Equivalent circuit of DC-DC converter during charging (b) Equivalent circuit of DC-DC converter during discharging process
5.7	Steady-state waveforms during power flow from HV side to LV side (a) Low voltage side voltage (kV) (b) High voltage side voltage (kV) (c) Submodule capacitor voltage (kV) (d) Transformer converter side current (kA) (e) Current through positive and negative wave shaping circuits (kA) (I_{wp1} and I_{wn1}) (f) Voltage output of positive and negative wave shaping circuit (kV) (V_{wp1} and V_{wn1}).
5.8	Dynamic operation of the converter during power flow from HV side to LV side with change in low voltage side voltage at $t=1.1$ sec (a) Low voltage side voltage (kV) (b) High voltage side voltage (kV) (c) Submodule capacitor voltage (kV) (d) High voltage DC side current (e) Load current (kA) (f) Voltage across the primary winding of the transformer (kV)
5.9	Steady-state waveforms during power flow from LV side to HV side (a) Low voltage side voltage (kV) (b) High voltage side voltage (kV) (c) Submodule capacitor voltage (kV) (d) Transformer converter side current (kA) (e) Current through positive and negative wave shaping circuits (I_{wp1} and I_{wn1}) (f) Voltage output of positive and negative wave shaping circuit (V_{wp1} and V_{wn1})
5.10	Dynamic operation of the converter during power flow from LV side to HV side with change in high voltage side voltage at $t=1.15$ sec (a) Low voltage side voltage (kV) (b) High voltage side voltage (kV) (c) Submodule capacitor voltage (kV) (d) Low voltage side current (e) Load current (kA) (f) Voltage across the primary winding of the transformer (kV)
5.11	Isolated DC-DC converter for exchanging power with Monopolar DC grid
5.12	WS_{P1} discharges to positive terminal of push-pull transformer and WS_{N1} charges from positive MVDC line
5.13	WS_{N1} discharges to negative terminal of push-pull transformer and WS_{P1} charges from positive MVDC line
5.14	Steady-state waveforms during power flow from HV side to LV side (a) High voltage side voltage (kV) (b) Low voltage side voltage (kV) (c) Submodule capacitor voltage (kV) (d) Output voltage of push-pull transformer (kV) (e) Voltage across positive wave shaping circuit-1 (kV) (f) Voltage across positive wave shaping circuit-2 (kV)
5.15	Dynamic operation of converter during power flow from HV side to LV side with change in low voltage side voltage at $t=1.1$ sec (a) Low voltage side voltage (kV) (b) High voltage side voltage (kV) (c)

	Submodule capacitor voltage (kV) (d) High voltage DC side current (e) Load current (kA) (f) Voltage across primary winding of transformer (kV)
5.16	Operation of the converter during (a) Stage-1-Positive cycle (b) Stage-1-Negative cycle and (c) Transition stage
5.17	Operation of the converter during (a) Stage-1-Positive cycle (b) Stage-1-Negative cycle and (c) Transition stage
5.18	Stages of operation of the converter
5.19	Stages of operation of the converter
5.20	Equivalent circuit diagram of the proposed converter during (a) charging and (b) discharging
5.21	Submodule voltage control of the proposed converter.
5.22	Hysteresis control of arm current.
5.23	(i) Steady-state waveforms of the converter (a) HVDC voltage (kV) (b) MVDC side voltage (kV) (c) Transformer voltage (kV) (d) Load current (kV) (ii) (a) Upper arm-1 voltage (b) Upper arm-2 voltage (c) Lower arm-1 voltage (d) Lower arm -2 voltage (iii) Dynamic operation of the converter (iii) Dynamic operation of converter during power flow from HV side to LV side by varying number of submodules inserted during discharging time (Submodule voltage kept constant) at t=1.0 sec (a) High voltage side voltage (kV) (b) MVDC Load side voltage (kV) (c) Submodule capacitor voltage (kV) (d) Current drawn from HVDC link (kA)
5.24	(i). Dynamic operation of converter during power flow from HV side to LV side with submodule reference voltage from 17kv to 15kV at t=1.0 sec (a) High voltage side voltage (kV) (b) MVDC Load side voltage (kV) (c) Submodule capacitor voltage (kV) (d) Current drawn from HVDC link (kA) (iii) Illustration of hysteresis control to draw constant current from HVDC link (a) High voltage side voltage (kV) (b) MVDC (Load side) voltage (kV) (c) Current drawn from HVDC link (kA) (d) Current through upper arm-1 (I_{p1}) and Upper arm-2 (I_{p2}) (kA).
5.25	Downscaled experimental prototype
5.26	Experimental results of the proposed converter: (i) (a) Input DC link voltage (b) Output DC voltage (c) positive arm voltage (d) negative arm voltage (ii) (a) positive arm input current (current through HV side DS) (b) positive arm output current (current through LV side DS) (c) positive arm current (d) Output DC voltage
5.27	(i) Sub-module capacitor voltages of the positive arm (ii) Dynamic operation of the converter during power flow from HV side to LV side by varying number of submodules inserted during charging and discharging time in three transition stage (a) input DC link voltage (b) output DC voltage (c) SM-1 capacitor voltage of positive arm (d) SM-1 capacitor voltage of negative arm
5.28	(i) Dynamic operation of the converter during power flow from HV side to LV side by varying number of submodules inserted during discharging time (i.e. from 3 SMs to 2 SMs) (a) input DC link voltage (b) output DC voltage (c) positive arm voltage (d) negative arm voltage (ii) zoomed version of (i).
6.1	AC and DC collection platforms for integration of renewable energy sources

6.2	Integration of AC collection platform with HVDC transmission line
6.3	Integration of AC collection platform with LCC HVDC system using MMC
6.4	Control of LCC HVDC system integrated with an AC collection platform
6.5	Flow chart illustrating start-up sequence of AC collection platform using MMC
6.6	Equivalent circuit of LCC HVDC system with MMC connected to AC collection platform during the fault
6.7	Start-up of AC collection platform using MMC in a LCC HVDC system (a) LCC HVDC transmission line voltage at the point of connection of AC collection platform using MMC (V_{dclcc}) and MMC DC Link voltage (V_{dct})- (kV) (b) Rectifier current (I_r) and Inverter current (I_i)- (kA) (c) Current injected by AC collection platform using MMC (d) MMC Submodule capacitor voltage (kV)
6.8	Power reversal of AC collection platform using MMC in HVDC system (a) Voltage at the point of connection of AC collection platform using MMC(kV) (b) Rectifier current (I_r) and Inverter current (I_i)- (kA) (c) Current from AC collection platform using MMC(kA) (d) Rectifier firing angle(a) and Inverter extinction angle(g)-(deg) (e) Power send by a rectifier (P_r) and Power received by inverter(P_i)(MW) (f) Power transferred to HVDC system by AC collection platform using MMC (MW)
6.9	DC fault in LCC HVDC system. (a) Voltage at the point of connection of AC collection platform using MMC (kV) (b) Rectifier current (I_r) and Inverter current (I_i)-(kA) (c) Current from AC collection platform using MMC(kA) (d) Fault current(kA) (e) Rectifier firing angle (a) and Inverter extinction angle(g)-(deg) (f) Submodule capacitor voltage(kV)
6.10	Direct Integration of renewable energy sources with MVDC network
6.11	Detailed configuration of the wind turbine integration scheme with MVDC system using new DC-DC converter.
6.12	Detailed configuration of the proposed scheme (One wind module connected to the Bipolar MVDC transmission corridor)
6.13	Detailed configuration of the proposed scheme (One wind module connected to the Bipolar MVDC transmission corridor)
6.14	Coordinated control of the MVDC system with DC collection platform
6.15	Variation of wind output power with wind speed (b) Illustration of power coefficient (C_p) vs tip speed ratio (λ)
6.16	Characteristics of solar PV panel. (b) Variation of solar power with insolation levels
6.17	Equivalent circuit of the proposed scheme during DC fault (Gate pulses to switches withdrawn)
6.18	DC fault in MVDC corridor no-1 (b) Isolation and transfer of power to MVDC corridor -2 by the action of DC switches
6.19	Wind speed (m/s) (b) Power output from wind turbine (MW) (c) Submodule capacitor voltage (kV) (d) Pitch angle

6.20	Characteristics of solar PV panel (a) Variation of power and current output with voltage (b) PV characteristics with different solar irradiation level
6.21	Fig 6.21. (a) Power output from solar cluster-1 (MW) (b) Submodule capacitor voltage (kV) (c) Duty cycle of MPPT DC-DC converter (kV) (d) Solar Insolation (W/m^2)
6.22	(a) DC breaker status (Red line:1-On,0-Off) and current through breaker (Blue line) (b) DC bypass breaker status (red line:1-On,0-Off) and current through breaker (blue line) (c) Submodule capacitor voltage (kV) (d) Power output from DC-DC converter (MW)
6.23	. (i) (a) Current through MVDC corridor-1 (kA) (b) Current through MVDC corridor-2 (kA) (c) Fault current (MW) (d) Current through bypass breakers (kA)
6.24	(ii) (a) Power output from module-1 (MW) (kA) (b) Power output from module-2 (c) Power through DC line-1 (MW) (d) Power through DC line-1 (MW)
7.1	Schemes presented in thesis to exchange power with HVDC transmission line

LIST OF TABLES

2.1	List of few VSC HVDC projects
2.2	List of HVDC schemes in India
2.3	Transmission corridor capacity
2.4	Comparison of Series and Parallel tapping scheme
2.5	Summary of converter requirements
3.1	Variation of voltage ratio with submodules
3.2	Required number of submodules to be inserted for various input voltages and the percentage error in the output voltage
3.3	HVDC System Parameters
3.4	Simulation parameters
3.5	Experimental parameters
4.1	Simulation parameters of MMC HVDC system
4.2	Simulation Parameters of DC-DC Converter
4.3	Experimental Parameters
4.4	Simulation parameters of MMC HVDC system
4.5	Simulation Parameters of DC-DC Converter
4.6	Experimental Parameters
4.7	Comparison of Topology-1 and Topology-2
5.1	Switching states during the operation of the DC-DC converter
5.2	Simulation Parameters
5.3	Switching states during the operation of the DC-DC converter with push-pull
5.4	Simulation Parameters
5.5	Switching states during the operation of the modified DC-DC converter
5.6	Simulation Parameters
6.1	Simulation parameters of LCC HVDC system
6.2	AC collection platform using MMC parameters
6.3	Simulation parameters
6.4	Windfarm simulation parameters
6.5	Solar cell simulation parameters

LIST OF ABBREVIATIONS

MMC	Modular Multilevel Converters
LV	Low Voltage
HV	High Voltage
DC	Direct Current
AC	Alternating Current
HVDC	High Voltage DC
MVDC	Medium Voltage DC
HVAC	High voltage AC
FACTS	Flexible Alternating Current Transmission System
STATCOM	Static Synchronous Compensator
PV	Photo Voltaic
BTB	Back-to-Back
VSC	Voltage Source Converter
VSI	Voltage Source Inverter
PWM	Pulse Width Modulation
GTO	Gate turn-off thyristor
IGCT	Integrated Gate-Commutated Thyristor
IGBT	Insulated Gate Bipolar Transistor
PI	Proportional-Integral
PF	Power Factor
DSP	Digital Signal Processor
IPM	Intelligent Power Module
PSCAD	Power Systems Computer Aided Design
EMTDC	Electromagnetic Transients including DC

LIST OF SYMBOLS

α	Alpha (firing angle)
γ	Gama (Extinction angle)
V_{HVDC}	HVDC voltage (V)
V_{MVDC}	MVDC voltage (V)
f	Fundamental frequency (Hz)
$n:1$	Transformer turns ratio